Factors controlling the photochemical degradation of methylmercury in coastal and oceanic waters

Supporting Information

Brian P. DiMento and Robert P. Mason

METHODS – Artificial sunlight

Early studies were conducted using 500 mL Teflon FEP bottles using buffered Milli-Q water (1 mM phosphate, pH 7), with initial CH_3Hg concentrations of 5 pM. Fluorescent lamps (Exo Terra Repti Glo 10.0; Total UV: 2.5 W m^{-2}, PAR: 14.5 W m^{-2}; see Fig. S1 for spectrum) were used in a low temperature incubator (28°C), and samples were exposed in duplicate for up to 48 hours. Experiments were done with and without added NO_3^- (1 mM) and Cl^- (up to 10 mM).

Later laboratory-based experiments utilized a 1 kW Oriel solar simulator with an AM1.0 air mass filter (Sciencetech Inc.). Quartz (250 and 500 mL, Technical Glass Products) round bottom flasks, chosen for their UV and visible spectral clarity, were used as reaction vessels. The output intensity from the solar simulator (Fig. S2) was strongly dependent on the distance from the light source, dropping ~10% per centimeter from the source. Total UV intensity at the center of the flask, selected for the calculation of rate constants, was 58.5 W m^{-2} (1011 W m^{-2} PAR), although it increased almost 50% to 85.2 W m^{-2} (1516 W m^{-2} PAR) at the top of the flask. Flasks were filled and capped to avoid headspace. PTFE coated magnetic stir bars were used to slowly mix solutions during experiments, and a shallow water bath was employed to maintain sample temperature (22±3°C). Methylmercury concentrations of 0.5 pM were used to keep experimental conditions as environmentally relevant as possible while still facilitating analysis throughout the course of the degradation. For experiments using the solar simulator, exposures were repeated in duplicate for a maximum duration of 80 minutes.

Natural water samples from NESB and WLIS were also used to examine the differences in CH_3Hg photodegradation rates in coastal and open ocean waters. In addition to experiments using the unlabeled CH_3Hg standard solution, in separate experiments these waters were amended with the stable isotope $CH_3{}^{199}Hg$ (2 pM added), with and without added NO_3^- (100 μM added) to test the effect of hydroxyl radical production from NO_3^- photolysis.

RESULTS AND DISCUSSION – Artificial Sunlight

Milli-Q

Preliminary studies in buffered Milli-Q water using fluorescent lamps showed enhanced degradation of CH_3Hg in the presence of NO_3^-, and no significant impact ($p > 0.05$; Table S3) of added Cl^- ions. While samples with added NO_3^- continued to show first order decay as concentrations approached zero, NO_3^- free samples stopped degrading after ~20% of the CH_3Hg had been lost. Despite this continued degradation, initial rates in the experiments involving NO_3^- were lower than rates in NO_3^- free samples (Table S1). In the absence of NO_3^-, it appears that insufficient concentrations of photochemically reactive species were present (possibly in the form of trace metal or organic impurities present in the reagents added) to sustain photodegradation.

At 10 mM Cl^-, the dominant species of CH_3Hg predicted is CH_3HgCl (83%; Fig. S4), predicted theoretically to be more difficult to degrade than CH_3HgOH, the primary form in the absence of chloride (Tossell, 1998). Decreasing the Cl^- concentration in these experiments did not impact the degradation rate (Table S1), however, suggesting that the inorganic speciation is not the primary control over the rate in this reaction pathway. The observation that the NO_3^- free samples stopped degrading suggests that the primary driver of degradation in these experiments was linked to the formation of reactive species in solution. Because of the absence of DOM in these experiments, we must be cautious in applying these results to natural waters where complexation of CH_3Hg is likely dominated by DOM.

Total UV rather than PAR intensities were used in the calculations to normalize rate constants because of the greater importance of UV radiation in CH_3Hg degradation (Lehnherr and St Louis, 2009), allowing for comparison between studies despite differing light intensities; however, while the Oriel solar simulator has an output spectrum similar to sunlight, the light output of these lamps is heavily weighted toward the UVB portion of the spectrum (Fig. S1). Because of the higher proportion of shorter high-energy wavelengths, the rates found under these conditions were higher than those found in the

natural waters.

Natural water

Degradation rates under simulated sunlight in coastal water from the WLIS were equal to rates in water from the NESB (Table S2). Experiments repeated with the stable isotope $CH_3{}^{199}Hg$, showed no significant change (Table S3) in degradation rate upon the addition of NO_3^-. Rates appeared to be faster using the higher concentration of stable isotopes versus the ambient spike, but the difference was only statistically significant (p = 0.007) at the WLIS site due to variability in the isotope studies. These spikes were added immediately before exposure, possibly indicating a potentially higher reactivity of non-equilibrated CH_3Hg standard, especially at higher concentrations. In later experiments, lower rates were determined under natural sunlight when the CH_3Hg was allowed to equilibrate with natural ligands in the water prior to exposure. Greater degradation rate constants determined in the isotope study could be a result of the higher CH_3Hg concentrations used, which were necessary to facilitate measurement on the ICP-MS. While our concentration dependence study using water from the Barn Island high organic carbon (BI-HOC) site did not reveal dramatically increased rate constants at higher CH_3Hg concentrations, these results may not apply to all water types, especially those with different sources and lower concentrations of DOM such as the WLIS and NESB sites.

Degradation rates in experiments using the solar simulator were also faster than those observed under natural sunlight, likely due to spectral differences between the two light sources. The rates were normalized to UV intensities in both cases, but the solar simulator had a much greater relative intensity of visible radiation. At equivalent UV intensities, the PAR output of the solar simulator was almost two times greater than the PAR intensity of sunlight. In addition, the light intensity varies greatly across the diameter of the flask under the solar simulator, increasing about 50% when moving from the center to the edge closest to the light source. Comparatively high rates versus natural sunlight could therefore indicate that the intensity at the point of the flask closest to the source might play a larger role in

determining the rate than the intensity at the midpoint (chosen for calculations), although stirring the samples could have alleviated this potential effect.

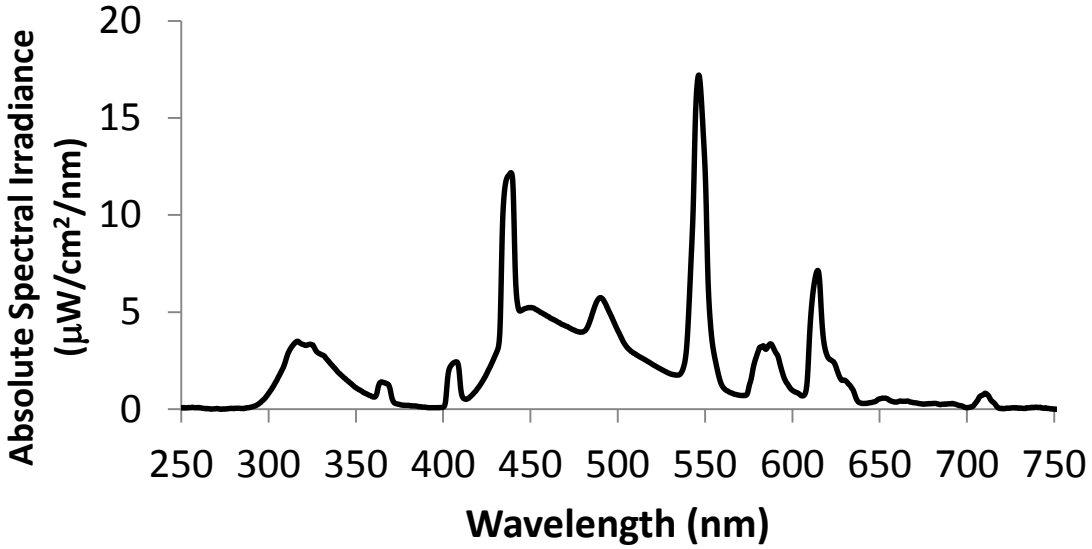

Fig. S1. Spectrum of Exo Terra Repti Glo 10.0 fluorescent lamps – Total UV: 2.5 W m^{-2}, PAR: 14.5 W m^{-2} – UVB : UVA : PAR % = 5.2 : 9.6 : 85.2 %.

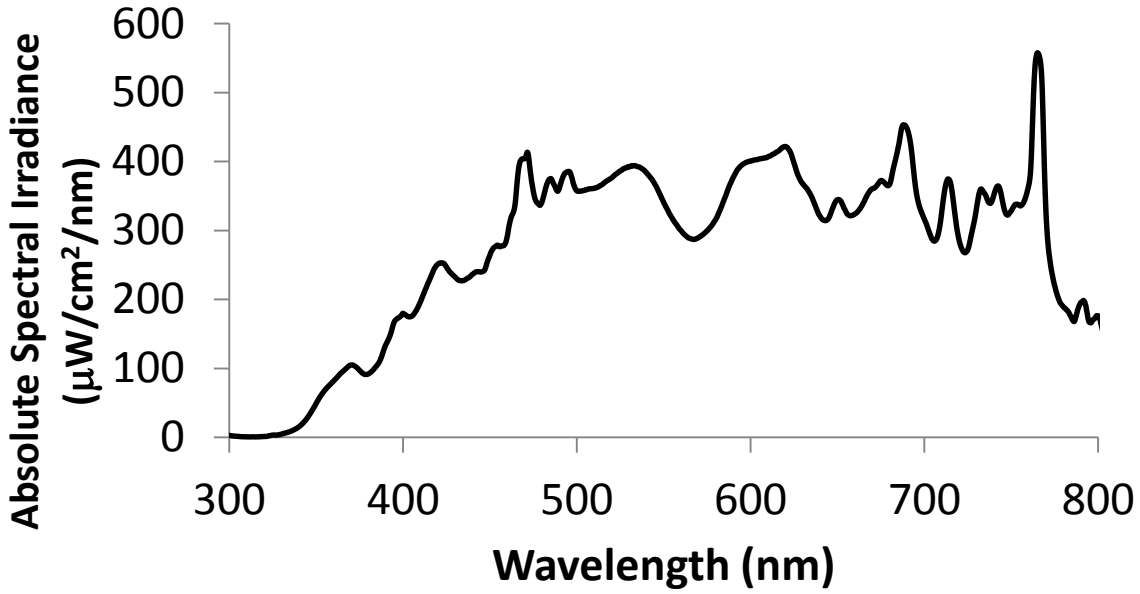

Fig. S2. Spectrum of 1 kW Oriel solar simulator with AM1.0 air mass filter – Total UV: 58.5 W m^{-2}, PAR: 1011 W m^{-2} – UVB : UVA : PAR % = 0.1 : 5.4 : 94.5 %.

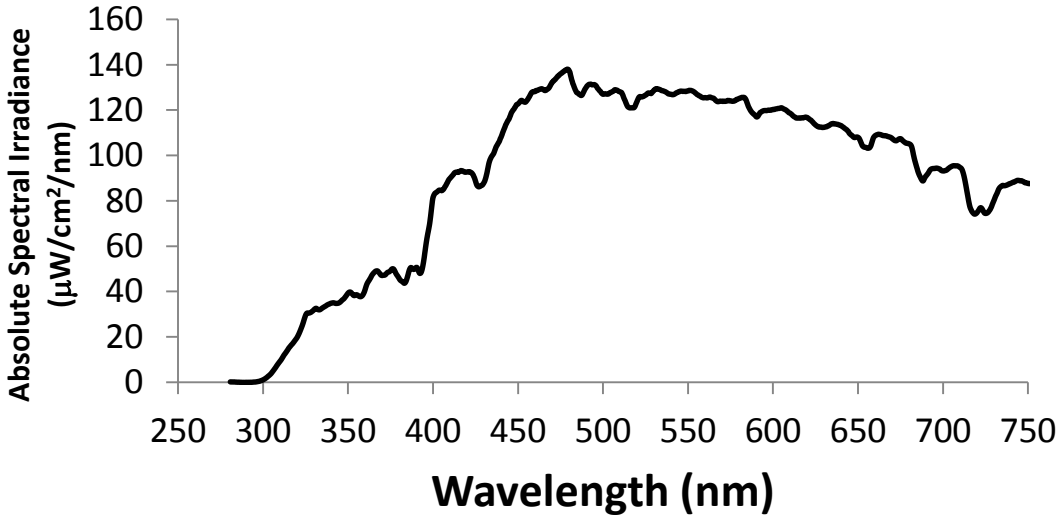

Fig. S3. Spectrum of natural sunlight at Avery Point, CT on June 30, 2016 at 15:01 Eastern Daylight Time (EDT) – Total UV: 35.9 W m^{-2}, PAR: 347 W m^{-2} – UVB : UVA : PAR % = 0.5 : 8.9 : 90.6 %.

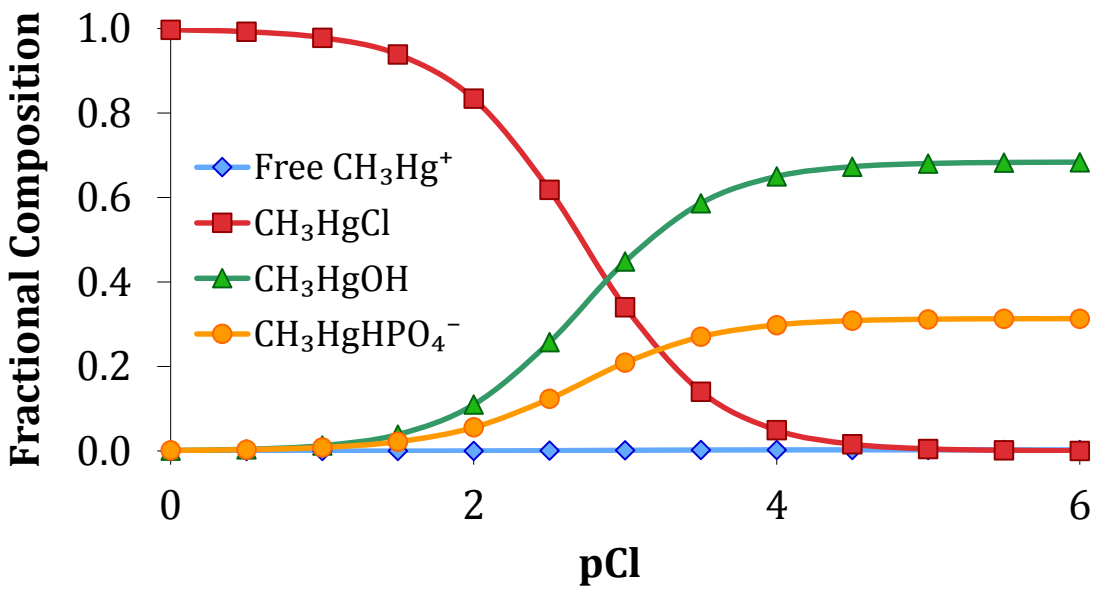

Fig. S4. Methylmercury (CH_3Hg) speciation in sample matrix – Milli-Q water with 1 mM phosphate (PO_4^{3-}) buffer (pH 7), 5 pM CH_3Hg, and varying chloride (Cl^-) concentrations (10^{-6} – 1 M).

Table S1

Rate constants (± standard error) for the degradation of methylmercury (CH_3Hg) in buffered Milli-Q water with additions of chloride (Cl^-) and/or nitrate (NO_3^-) under fluorescent reptile lamps.

$[Cl^-]$ (mM)	$[NO_3^-]$ (mM)	Rate Constant (day^{-1})
0	0	8.52 ± 2.00
1	0	10.97 ± 1.55
10	0	7.02 ± 3.16
0	1	4.54 ± 0.18
10	1	4.27 ± 0.45

Table S2

Photochemical degradation rate constants (± standard error) and other ancillary parameters for Western Long Island Sound (LIS) and New England Shelf Break sites, with and without added nitrate (NO_3^-).

Location	Trial	Date	Salinity (ppt)	DOC (µM)	NO_3^- (µM)	SUVA (L mg^{-1} m^{-1})	Rate Constant (day^{-1})
Western LIS	CH_3Hg	9/14/14	27.2	138	1.3	1.8	2.27 ± 0.51
	$CH_3{}^{199}Hg$	9/16/14					6.82 ± 1.23
	$CH_3{}^{199}Hg + NO_3^-$	9/16/14					3.82 ± 0.93
Shelf Break	CH_3Hg	9/15/14	35.6	85	<0.5	0.9	2.28 ± 0.58
	$CH_3{}^{199}Hg$	9/15/14					4.67 ± 3.40
	$CH_3{}^{199}Hg + NO_3^-$	9/16/14					4.69 ± 1.89

Table S3

P-values for the regression analysis of rate constants in this study. Statistically significant differences ($p < 0.05$) are highlighted in pink, while marginally significant differences ($0.05 < p < 0.1$) are highlighted in blue. (**A)** Degradation of methylmercury (CH_3Hg) under fluorescent lamps in buffered Milli-Q water with additions of chloride (Cl^-) and/or nitrate (NO_3^-). (**B)** Degradation of CH_3Hg in Western Long Island Sound (WLIS) and New England Shelf Break (NESB) sites under the solar simulator, with and without added nitrate (NO_3^-). (**C)** Degradation of CH_3Hg under natural sunlight across a range of coastal and oceanic sites. (**D+E)** Degradation of CH_3Hg under natural sunlight illustrating the effect of Cl^- additions to Shetucket River water and bromide (Br^-) additions to coastal seawater from Avery Point.

(A)	**[Cl^-], [NO_3^-] (mM)**	0, 0	1, 0	10, 0	0, 1	10, 1
	0, 0		0.355	0.696	0.065	0.058
	1, 0			0.290	0.001	0.002
	10, 0				0.446	0.405
	0, 1					0.575
	10, 1					

(B) Site	WLIS	WLIS $CH_3^{199}Hg$	WLIS $CH_3^{199}Hg + NO_3^-$	NESB	NESB $CH_3^{199}Hg$	NESB $CH_3^{199}Hg + NO_3^-$
WLIS		0.007	0.610	0.984	0.500	0.245
WLIS $CH_3^{199}Hg$			0.369	0.009	0.570	0.373
WLIS $CH_3^{199}Hg + NO_3^-$				0.616	0.853	0.808
NESB					0.506	0.255
NESB $CH_3^{199}Hg$						0.998
NESB $CH_3^{199}Hg + NO_3^-$						

(C) Site	DE - Slaughter Beach	NJ - Berry's Creek	CT - Barn Island LOC	CT - Barn Island HOC	CT - Avery Point	CT - Shetucket River	ME - Sea Mist	ME - Drakes Island Beach	Eastern LIS	Bering Strait	Arctic Ocean	Pacific Ocean
DE - Slaughter Beach		0.420	0.228	0.177	0.594	0.314	0.475	0.267	0.482	0.170	0.535	0.354
NJ - Berry's Creek			0.108	0.095	0.268	0.738	0.811	0.136	0.205	0.866	0.935	0.761
CT - Barn Island LOC				0.891	0.720	0.012	0.077	0.660	0.375	0.013	0.254	0.023
CT - Barn Island HOC					0.750	0.000	0.052	0.597	0.207	0.004	0.255	0.003
CT - Avery Point						0.211	0.297	0.540	0.894	0.118	0.385	0.218

CT - Shetucket River				0.950	0.116	0.016	0.356	0.767	0.954
ME - Sea Mist					0.135	0.158	0.587	0.803	0.972
ME - Drakes Island Beach						0.398	0.064	0.227	0.122
Eastern LIS							0.026	0.397	0.060
Bering Strait								0.983	0.423
Arctic Ocean									0.777
Pacific Ocean									

(D)	**[Cl-] (mM)**	~0.3	34	330
	~0.3		0.200	0.018
	34			0.310
	330			

(E)	**[Br-] (mM)**	~0.8	7	60
	~0.8		0.068	0.077
	7			0.787
	60			